American Mineralogist, Volume 73, pages 1346–1354, 1988

Optical (diffuse reflectance) and Mössbauer spectroscopic study of nontronite and related Fe-bearing smectites

DAVID M. SHERMAN, NORMA VERGO
U.S. Geological Survey, Mail Stop 964, Box 25046, Denver Federal Center, Denver, Colorado 80225, U.S.A.

ABSTRACT

Near-ultraviolet to near-infrared optical (diffuse reflectance) spectra of several nontronites and related Fe-bearing smectites [(Fe^{2+},Fe^{3+})-bearing saponite and (Fe^{2+},Fe^{3+})-bearing montmorillonite] are presented and interpreted. Mössbauer spectra at 298 K are also presented to help interpret the optical spectra. The optical spectra of nontronites are dominated by the ligand field transitions of Fe^{3+} in octahedral coordination sites. Values for the ligand-field-theory parameters $10Dq$, B, and C, are 15050 cm^{-1}, 614 cm^{-1}, and 3268 cm^{-1}, respectively. In addition to the ligand field transitions of single Fe^{3+} cations, a broad absorption band centered near 22000 cm^{-1} is observed that may be due to the simultaneous excitation of two Fe^{3+} cations to the $^4T_{1g}(^4G)$ state. Such "pair excitations" have been proposed in the spectra of other Fe^{3+}-bearing minerals in which next-nearest-neighbor Fe^{3+} cations are magnetically coupled. Alternatively, this band may represent excitations to the $^2A_{2g}$ and $^2T_{1g}$ ligand field states.

For most samples, the amount of tetrahedrally coordinated Fe^{3+} was below that detectable by Mössbauer spectroscopy (1–3% of total Fe). However, the optical spectra of all of the nontronites show an absorption band near 23000 cm^{-1}. This band is assigned to the $^6A_1 \rightarrow {}^4E,{}^4A_1$ transition of tetrahedrally coordinated Fe^{3+}.

The optical spectra of mixed-valence Fe-bearing smectites [(Fe^{2+},Fe^{3+})-bearing saponite and (Fe^{2+},Fe^{3+})-bearing montmorillonite] show a broad absorption band at 14000–15000 cm^{-1} owing to $Fe^{2+} \rightarrow Fe^{3+}$ charge transfer.

INTRODUCTION

Nontronite $(Ca,Na)_{0.66}Fe_4Si_{7.34}Al_{0.66}O_{20}(OH)_4 \cdot nH_2O$, is a 2:1 sheet silicate that forms during the hydrothermal alteration and surface weathering of mafic rocks. It is often a major component of terrestrial soils and sediments and also may be present as a surface mineral on Mars. Understanding the optical (visible to near-infrared) spectra of Fe-bearing smectites is needed to help interpret the surface reflectance spectra of the Earth and Mars. In addition, visible to near-infrared spectra can aprovide some insight into the crystal chemistry and electronic structures of these minerals. Such information is needed to understand the complex chemistry of Fe-bearing smectites in sediments and natural waters. There have been several previous investigations on the optical spectra of Fe^{3+}-bearing smectites. Karickhoff and Bailey (1973) presented the spectrum of nontronite, but because their spectra did not extend into the near-infrared, some of the bands were incorrectly assigned. Singer (1982) presented spectra of nontronite to help interpret the spectrum of Mars but did not make detailed band assignments. In this paper, we present and interpret the visible and near-infrared optical (diffuse reflectance) spectra of nontronites covering a wide range of composition.

Fe can occupy several different crystallographic sites in nontronite and other smectites. Most of the Fe occupies sites in the octahedral sheet. However, some Fe^{3+} may replace Si or Al in tetrahedral sites, and Fe may occur as an interlayer species. In the optical spectrum, each species of Fe will give rise to its own set of absorption bands owing to the Fe ligand field transitions. If both Fe^{2+} and Fe^{3+} are present and occupying adjacent sites, additional absorption bands will result from $Fe^{2+} \rightarrow Fe^{3+}$ charge-transfer transitions. It follows that any independent knowledge of a mineral's crystal chemistry can greatly simplify the interpretation of its optical spectrum. For this reason, we have also obtained Mössbauer spectra to investigate the crystal chemistry of Fe in the nontronite and Fe-bearing smectite samples. There have been several Mössbauer studies directed toward understanding the site occupancy of Fe in smectites (e.g., Cardile and Johnston, 1985; Besson et al., 1983; Bonnin et al., 1985; Helsen and Goodman, 1983), and the results obtained here will be compared with these earlier studies.

EXPERIMENTAL DETAILS

Methods

The clay samples were dispersed in distilled water using an ultrasonic probe and were size-separated by centrifugation to yield the <2-μm size fraction. X-ray diffractometer scans of random orientation mounts of the <2-μm size fraction were done using Ni-filtered Cu radiation. This size fraction, which should contain only clay particles, was then oriented by centrifugation

0003–004X/88/1112–1346$02.00

TABLE 1. Sample descriptions

Sample	Description	Locality	Comments
NB1	Nontronite-beidellite	Spokane, Washington	Sample no. 58 in Ross and Hendricks (1945)
N2	Nontronite	Sandy Ridge, North Carolina	Sample no. 65 in Ross and Hendricks (1945)
N3	Nontronite	Garfield, Washington	API H-33A
N4	Nontronite	Tirschenreuth, Bayern, Germany	National Museum of Natural History no. R4885
N5	Nontronite	Colfax, Washington	
S1	(Fe^{2+},Fe^{3+})-bearing saponite	Grande Rone Formation, Hanford, Washington	
M1	(Fe^{2+},Fe^{3+})-bearing montmorillonite	Hanaoka Mine, Akita, Japan	National Museum of Natural History no. 106061

on a ceramic tile following the methods of Kinter and Diamond (1956). X-ray diffraction patterns were run on untreated, glycol-saturated, K-saturated, Mg-saturated, and heat-treated (300 °C for 2 and 550 °C for 2 h) samples. The clay samples were saturated with Mg and K using the procedures outlined in Jackson (1956). Glycol solvation was achieved by direct application of ethylene glycol to the clay on the ceramic tile.

Chemical compositions of the samples were obtained using inductively coupled plasma emission spectroscopy at the U.S. Geological Survey.

Mössbauer spectra were obtained at 298 K using a 20-mCi ^{57}Co source in a Rh matrix. The velocity scale was calibrated relative to Fe^0. The spectra were fit to a sum of their component Lorentzian peaks. The widths and areas of component peaks within a given quadrupole doublet were constrained to be equal. Different quadrupole doublets, however, had different peak widths.

Diffuse-reflectance spectra were obtained using a Beckman Acta MVII spectrometer with a halon-coated integrating sphere. The spectra were converted to the Kubulka-Munk remission function,

$$F(R) = [(1 - R)^2/2R] \approx k/s,$$

where R is absolute reflectance, k is the absorption coefficient, and s is the scattering coefficient. To the extent that the scattering coefficient is approximately independent of wavelength, the Kubulka-Munk remission function will be equivalent to the absorption spectrum. The spectra were then fit to a set of unconstrained Gaussian peaks on a polynomial baseline.

SAMPLE DESCRIPTIONS

A list of the samples investigated and their localities is given in Table 1. From the X-ray diffraction results (Table 2) and the structural formulae (Table 3), all of the samples are found to be pure smectite clay. The octahedral-layer compositions of the samples are plotted on a Al-Fe-Mg diagram in Figure 1.

Nontronite and nontronite-biedellite

The compositions of samples N2, N3, N4, and N5 fall close to that of hypothoetical end-member nontronite, and the d_{010} spacings (obtained from d_{060} measurements) in these samples range from 9.06 to 9.18 Å. The structural formulae of all of these samples (except N2) indicate the presence of tetrahedrally coordinated Fe^{3+}.

Sample NB1 is intermediate between nontronite and biedellite. The d_{010} spacing of 9.06 Å is smaller than that of nontronite and reflects the large Al content of the octahedral layer.

(Fe^{2+},Fe^{3+})-bearing saponite

The composition of sample S1 is between hisingerite and Fe-bearing saponite using the definitions of Brigatti (1982). However, the phase hisingerite is considered to be nearly X-ray amorphous (Eggleton et al., 1983). Sample S1 is similar to the oxidized Fe-rich saponites described by Kohyama et al. (1973). The d_{010} spacing is 9.18 Å owing to the large Mg^{2+} content of the octahedral layer. Unlike the nontronites, which are pale apple-green to greenish-yellow, the color of sample S1 is dark brown.

TABLE 2. d spacings of samples

	NB1	N2	N3	N4	N5	S1	M1
Air dried (001)	15.1	15.0	15.0	13.6	14.5	15.0	15.2
Air dried (060)	1.51	1.52	1.52	1.53	1.52	1.53	1.50
Glycol (001)	17.1	17.3	17.3	16.9	17.0	17.6	17.0
K-saturated (001)	13.1	16.7	11.9	15.2	12.1	12.8	12.1
Mg-saturated (001)	17.3	15.0	15.0	14.6	14.7	13.4	14.5
Heat at 300 °C for 2 h (001)	11.8	10.4	10.0	10.4	10.4	10.0	11.9
Heat at 550 °C for 2 h	10.4	10.1	10.0	9.6	10.2	9.9	10.6

TABLE 3. Sample compositions* and structural formulae

	NB1	N2	N3	N4	N5	S1	M1
SiO_2	44.3	41.4	40.8	48.8	41.4	43.0	50.1
Al_2O_3	12.8	8.4	4.1	0.7	4.1	3.3	18.2
Fe_2O_3	20.4	27.9	30.2	32.4	30.4	22.1	4.8
MgO	1.00	0.61	0.82	1.40	0.83	10.2	4.00
CaO	1.37	0.77	2.20	1.40	2.20	1.90	2.10
Na_2O	0.00	0.29	0.20	0.11	0.21	0.47	0.24
K_2O	0.09	0.03	0.03	0.03	0.02	0.30	2.80
TiO_2	1.72	0.10	0.12	0.10	0.08	0.16	0.33
P_2O_5	0.00	0.01	0.02	0.01	0.02	0.01	0.09
H_2O+		11.4	11.3	7.8	10.4	8.9	9.2
H_2O-		8.7	11.7	7.1	10.8	9.6	6.7
Total		99.7	101.5	99.9	100.5	100.0	98.6
Tetrahedral sites							
Si	6.97	6.93	7.07	7.71	7.10	7.03	7.43
Al	1.03	1.07	0.84	0.13	0.83	0.63	0.58
Fe^{3+}	0.00	0.00	0.09	0.16	0.07	0.36	0.00
Octahedral sites							
Al	1.34	0.59	0.00	0.00	0.00	0.00	2.60
Fe^{3+}	2.41	3.51	3.94	3.85	3.85	2.23	0.47
Fe^{2+}	0.00	0.00	0.00	0.00	0.00	0.14	0.07
Mg	0.24	0.15	0.21	0.33	0.21	2.49	0.88
Ti	0.21	0.01	0.02	0.01	0.00	0.02	0.04
Interlayer sites							
Ca	0.23	0.14	0.41	0.23	0.40	0.33	0.33
Na	0.00	0.09	0.07	0.33	0.07	0.15	0.07
K	0.02	0.01	0.01	0.01	0.00	0.06	0.53

* Analysts: NB1: B. Scott (U.S. Geological Survey) using X-ray fluorescence. All other samples: H. Smith (U.S. Geological Survey) using inductively coupled plasma emission spectroscopy. Fe^{2+}/Fe^{3+} values are estimated from Mössbauer spectra (Table 4).

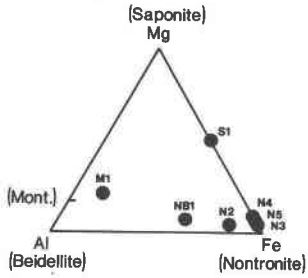

Fig. 1. Octahedral-layer compositions of the samples investigated.

(Fe^{2+},Fe^{3+})-bearing montmorillonite

Sample M1 is a montmorillonite that contains enough Fe to make it pale green rather than white. The d_{010} spacing is 9.00, and the Fe content is only 0.54 cations per 22 oxygens.

Mössbauer spectra

Nontronites and nontronite-beidellite

The Mössbauer spectra of the nontronites (Figs. 2a–5a) and nontronite-beidellite (Fig. 6a) were fit to two quadrupole doublets corresponding to Fe^{3+} cations in two different octahedral sites. For samples NB1 and N4, an additional doublet, corresponding to tetrahedrally coordinated Fe^{3+}, was included. The results of the fitting procedures are summarized in Table 4. The relative areas of the tetrahedral Fe^{3+} doublets are in qualitative agreement with the fraction of tetrahedral Fe suggested by the structural formula (less than 4% of total Fe). Note, however, that the structural formulae were calculated by assuming that Al enters the tetrahedral layer before Fe. Moreover, small amounts (less than 4% of total Fe) of tetrahedrally coordinated Fe^{3+} are difficult to measure accurately using Mössbauer spectroscopy. Only small improvements in the goodness-of-fit parameter χ^2 resulted by including the tetrahedral Fe^{3+} quadrupole doublet.

None of the samples show evidence of iron oxides (e.g., hematite) or oxide-hydroxides (e.g., goethite, lepidocrocite) in the Mössbauer spectra. Concentrations of such impurities on the order of 2% would probably not be detectable by Mössbauer spectroscopy (at least over the velocity range used) but would show up in the diffuse-reflectance spectra (e.g., Singer, 1982). As pointed out by Murad (1987), room-temperature Mössbauer spectra may not necessarily yield a six-line spectrum if iron oxides and oxide-hydroxides are present. Such phases may be either paramagnetic (as in the case of lepidocrocite) or of sufficiently poor crystallinity to be superparamagnetic. Low-temperature (e.g., 77 K) spectra must be taken if iron oxides are to be detected by Mössbauer spectra alone.

The Garfield nontronite (sample N3) has been well studied and provides a useful standard for comparison. Bonnin et al. (1985) have presented a detailed spectroscopic investigation of its site occupancy. Their Mössbauer results are in excellent agreement with those obtained here and also indicate that tetrahedral Fe^{3+} is less than 1–2% of the total Fe. The structural formula derived from the chemical analysis presented here assigns 2% of the Fe to the tetrahedral site, but this assignment may be simply due to error in the chemical analysis.

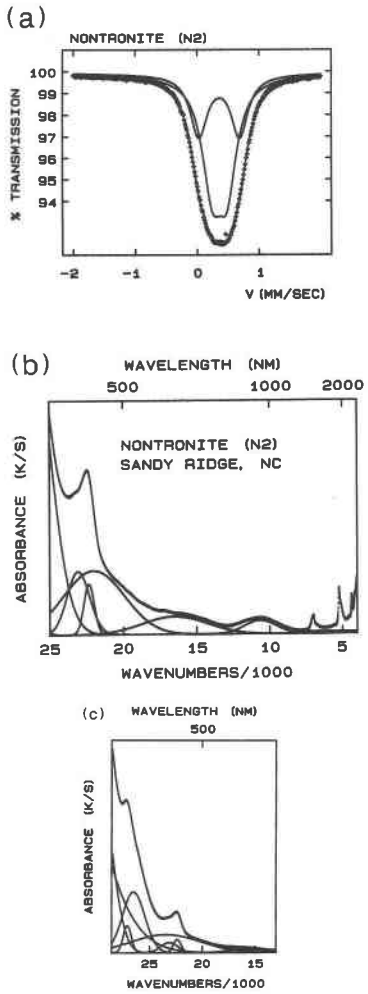

Fig. 2. (**a**) Room-temperature (298 K) Mössbauer spectrum of nontronite sample N2 together with the calculated fit and the component doublets (solid lines). The calculated fit is to two kinds of octahedrally coordinated Fe^{3+}. The velocity scale is relative to Fe^0 (α-Fe). (**b, c**) Optical spectrum of nontronite sample N2 together with its Gaussian model fit. Most of the absorption bands are due to the ligand field transitions of octahedrally coordinated Fe^{3+}. An additional band near 21890 cm^{-1} is due to either the simultaneous excitation of two Fe^{3+} cations to the $^4T_{1g}$ state or to the $^6A_{1g} \rightarrow {}^2T_{1g},{}^2A_{2g}$ ligand field transition. Finally, a band near 23000 cm^{-1} is attributed to tetrahedrally coordinated Fe^{3+}.

There is some uncertainty regarding the crystal-chemical interpretation of the two octahedral Fe^{3+} quadrupole doublets. The area fractions of the inner and outer octahedral Fe^{3+} doublets are roughly ⅔ and ⅓, respectively, leading to the idea that the two doublets might correspond to *cis*-$FeO_4(OH)_2$ (inner doublet) and *trans*-

$FeO_4(OH)_2$ (outer doublet) coordination sites and that Fe^{3+} cations are completely disordered over the two sites. A simple point-charge calculation of the electric-field-gradient tensor predicts that the quadrupole splitting of a *trans*-$FeO_4(OH)_2$ site should be 2.0 times that of a *cis*-$FeO_4(OH)_2$ site. The observed quadrupole splitting of the outer doublet is 2.3–2.7 times that of the inner doublet, in qualitative agreement with prediction. Bonnin et al. (1985) have shown from ^1H NMR spectra that there are two nonequivalent hydroxyl groups in the octahedral layer that can be explained if Fe is occupying both the *cis*- and *trans*-octahedral sites. Based on electron-diffraction measurements, Besson et al. (1983) and Mering and Oberlin (1967) have argued that in nontronite the *trans*-$FeO_4(OH)_2$ octahedral sites are vacant. The two quadrupole doublets observed in the Mössbauer spectrum correspond to two different *cis*- octahedral sites. This idea is debatable since it is based on interpreting the electron-diffraction pattern of nontronite using kinematic theory. It has been argued by Mering and Oberlin (1967), however, that dynamical effects on the electron-diffraction pattern can be avoided by looking only at crystals that are one layer thick (so that the plane group of the layer rather than the space group of the crystal is determined).

To explain how Fe^{3+} cations in only *cis*-$FeO_4(OH)_2$ octahedral sites can give two quadrupole doublets, Goodman (1978) invoked the electrostatic effect of Fe^{3+} in the tetrahedral sites on the electric-field gradient at the *cis*-$FeO_4(OH)_2$ site. Cardile and Johnston (1985) and Johnston and Cardile (1985) have argued that, in addition to tetrahedral Fe^{3+}, interlayer cations (Ca^{2+}, K^+, Na^+) exert a sufficient electrostatic effect to account for the second quadrupole doublet. Based on point-charge electrostatic calculations of the quadrupole splitting, Daynyak and Drits (1987) explained the two quadrupole doublets as reflecting [4Si] (for the inner doublet) and [3Si1Al] (for the outer doublet) configurations in the tetrahedral layer surrounding the octahedral Fe^{3+} site. The models invoking next-nearest-neighbor cations to account for two quadrupole doublets imply that the area ratios of the two doublets would vary with the interlayer and tetrahedral-layer compositions.

Our results show, however, there is no compositional effect on the relative areas of the inner- and outer-quadrupole doublets. Sample N4 has a much lower Al + Fe content in the tetrahedral layer, yet its Mössbauer spectrum is nearly identical to those of samples NB1, N2, N3, and N5. One would expect the outer quadrupole doublet to have a much smaller relative area in the Mössbauer spectrum of sample N4. More work on understanding the octahedral-layer site occupancies is needed to determine which interpretation of the Mössbauer spectra and electron-diffraction data is correct.

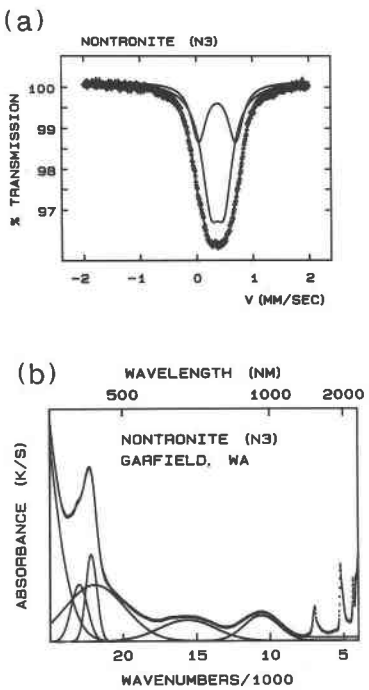

Fig. 3. (a) Mössbauer spectrum of nontronite sample N3 showing fit to two kinds of octahedrally coordinated Fe^{3+}. (b) Optical spectrum of nontronite sample N3 together with its calculated fit. The band assignments are as in Fig. 2b.

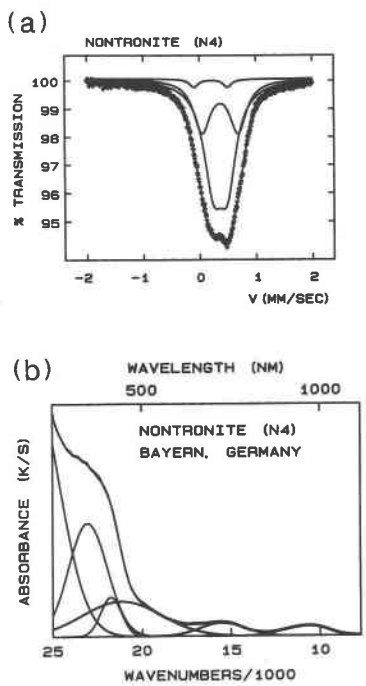

Fig. 4. (a) Mössbauer spectrum of nontronite sample N4 showing fit to two kinds of octahedrally coordinated Fe^{3+} and a small fraction (2.7% of total Fe) of Fe^{3+} in tetrahedral coordination. (b) Optical spectrum of nontronite sample N4 together with its calculated fit. The band assignments are as in Fig. 2b. Owing to the greater fraction of tetrahedral Fe^{3+} in this sample, the band near 23000 is more intense.

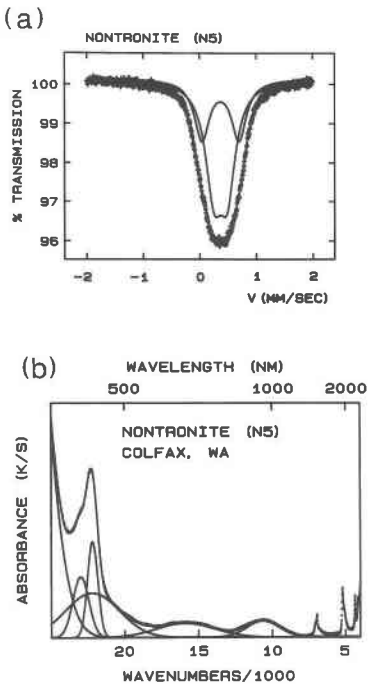

Fig. 5. (a) Mössbauer spectrum of nontronite sample N5 showing fit to two kinds of octahedrally coordinated Fe^{3+}. (b) Optical spectrum of nontronite sample N5 together with its calculated fit. The band assignments are as in Fig. 2b.

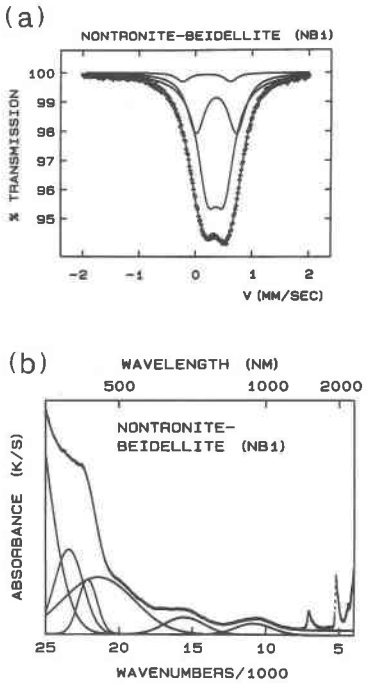

Fig. 6. (a) Mössbauer spectrum of nontronite-beidellite sample NB1. The Mössbauer spectrum is similar to that of the nontronites except that the quadrupole splittings of the two Fe^{3+} doublets are larger. Fe^{3+} cations in montmorillonite give doublets with even larger quadrupole splittings. Although the structural formula of this sample indicates no tetrahedrally coordinated Fe^{3+}, the Mössbauer spectrum was improved by including a doublet corresponding to tetrahedrally coordinated Fe^{3+} (3.6% of the total Fe). (b) Optical spectrum of nontronite-beidellite sample (NB1) showing Fe^{3+} absorption bands with the same energies as those in end-member nontronite. The band energies, therefore, imply that the Fe–O bond length in the octahedral sheet of this phase is the same as that in nontronite. The band at 23000 cm^{-1} that is attributed to tetrahedrally coordinated Fe^{3+} is also found in the spectrum of this sample in agreement with the Mössbauer results.

(Fe^{2+},Fe^{3+})-bearing saponite

The Mössbauer spectrum of the Fe-bearing saponite (Fig. 7a) is more complex than the spectra of the nontronites. In addition to two octahedral Fe^{3+} doublets, there are smaller doublets due to tetrahedrally coordinated Fe^{3+} and octahedrally coordinated Fe^{2+}. The fraction of Fe in tetrahedral coordination is estimated to be 8.8% from the Mössbauer spectrum and 13.2% from the structural formula.

(Fe^{2+},Fe^{3+})-bearing montmorillonite

The Mössbauer spectrum of this sample is given in Figure 8a, and the calculated Mössbauer parameters are given in Table 4. In addition to two kinds of octahedrally coordinated Fe^{3+}, there are two kinds of octahedral Fe^{2+} resolvable in the spectra. By analogy with the Mössbauer spectra of trioctahedral-sheet silicates, the two Fe^{2+} doublets most likely represent Fe^{2+} cations in *cis*- and *trans*-$FeO_4(OH)_2$ sites in the octahedral sheet. Note that neither of the two Fe^{2+} doublets can be due to interlayer Fe^{2+} since, at 298 K, the recoil-free fraction of interlayer Fe^{2+} would be too low to give a measurable absorption (Helsen and Goodman, 1983).

Optical (diffuse reflectance) spectra

Nontronite and nontronite-beidellite

The Mössbauer results on the nontronites and nontronite-beidellite show, as expected, that nearly all of the Fe occurs as octahedrally coordinated Fe^{3+}. None of the samples contain any detectable Fe^{2+}, but most samples show some evidence for small amounts of tetrahedrally coordinated Fe^{3+}. The optical spectra of the nontronites (Figs. 2b–5b) and the nontronite-beidellite (Fig. 6b) are dominated by absorption bands due to the ligand field transitions of octahedrally coordinated Fe^{3+}. The energies of the component absorption bands in the optical spectra, together with their proposed assignments, are given in Table 5.

A number of sharp bands occur near 4000–7000 cm^{-1}. These bands are due to the overtones and combinations of structural OH and interlayer H_2O vibrational modes. These bands were not included in the curve-fitting procedure since they are already well resolved and do not interfere with the Fe^{3+} ligand field bands.

From the energies of the ligand field transitions, values for $10Dq$, B, and C are calculated to be 15050 cm^{-1}, and

TABLE 4. Mössbauer parameters

	NB1	N2	N3	N4	N5	S1	M1
				Fe^{3+} Oct(A)			
I.S.	0.37	0.36	0.37	0.36	0.37	0.35	0.37
Q.S.	0.30	0.24	0.24	0.25	0.23	0.81	0.53
F.W.H.M.	0.44	0.48	0.38	0.40	0.46	0.48	0.28
% Area	63.9	65.5	67.5	64.5	65.1	55.6	59.5
				Fe^{3+} Oct(B)			
I.S.	0.37	0.36	0.37	0.36	0.37	0.37	0.30
Q.S.	0.71	0.66	0.66	0.64	0.65	1.35	0.88
F.W.H.M.	0.38	0.32	0.32	0.36	0.32	0.44	0.40
% Area	32.5	34.4	32.5	32.8	34.9	29.7	27.9
				Fe^{3+} (Tet)			
I.S.	0.19	—	—	0.20	—	0.24	—
Q.S.	0.84	—	—	0.60	—	0.54	—
F.W.H.M.	0.28	—	—	0.20	—	0.36	—
% Area	3.6	—	—	2.7	—	8.6	—
				Fe^{2+} (Oct)			
I.S.	—	—	—	—	—	1.13	1.34, 1.14
Q.S.	—	—	—	—	—	2.65	2.43, 1.27
F.W.H.M.	—	—	—	—	—	0.28	0.24, 0.21
% Area	—	—	—	—	—	6.1	9.0, 3.6
Reduced χ^2	1.0	2.8	0.9	1.5	0.8	1.7	1.0

Note: I.S. = Isomer shift relative to α-Fe, Q.S. = quadrupole splitting, F.W.H.M. = full width of line at half its maximum intensity.

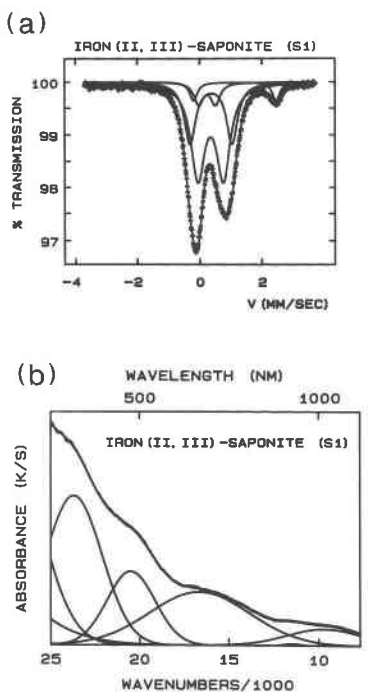

Fig. 7. (a) Mössbauer spectrum of Fe-bearing saponite sample S1. In addition to the two quadrupole doublets corresponding to octahedrally coordinated Fe^{3+}, there are weaker doublets corresponding to tetrahedrally coordinated Fe^{3+} and octahedrally coordinated Fe^{2+}. (b) Optical spectrum of Fe-bearing saponite sample S1. The small Fe^{2+} content gives Fe^{2+} ligand field absorption bands near 10000 cm^{-1}. A broad band near 15000 cm^{-1} is attributed to $Fe^{2+} \rightarrow Fe^{3+}$ charge transfer. Consistent with the large amount of tetrahedrally coordinated Fe^{3+} in this sample, a strong band is found near 23000 cm^{-1} that is assigned to the $^6A_1 \rightarrow {}^4E,{}^4A_1$ transition of tetrahedral Fe^{3+}. The presence of that band makes this sample dark brown rather than the green color expected for a mixed-valent smectite.

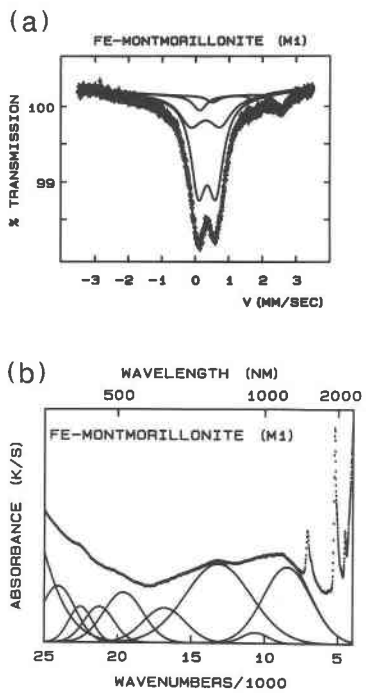

Fig. 8. (a) Mössbauer spectrum of Fe-bearing montmorillonite showing doublets due to octahedrally coordinated Fe^{3+} and Fe^{2+}. (b) Optical spectrum of Fe-bearing montmorillonite sample M1. The sharp bands near 7100 cm^{-1} are due to vibrational overtones of structural OH and interlayer water. The bands near 9000 and 10000 cm^{-1} are due to Fe^{2+}. The strong, broad band near 14000 cm^{-1} is due to $Fe^{2+} \rightarrow Fe^{3+}$ intervalence charge transfer. The origins of the bands at higher energies are unknown but may be due to exchange-enhanced transitions to the triplet Fe^{2+} ligand field states. There is no evidence for any of the Fe^{3+} ligand field bands even though most of the Fe in this sample is in the Fe^{3+} oxidation state.

TABLE 5. Band positions in optical spectra of nontronites and nontronite-beidellite

Transition	Energy (in cm^{-1})				
	NB1	N2	N3	N4	N5
Octahedral Fe^{3+}					
$^6A_{1g} \rightarrow {}^4T_{1g}$	10791	10692	10592	10730	10640
$^6A_{1g} \rightarrow {}^4T_{2g}$	15550	15775	15480	15420	15760
$2[^6A_{1g}] \rightarrow 2[^4T_{1g}](?)$*	21360	22300	21710	22090	21980
$^6A_{1g} \rightarrow {}^4E_g, {}^4A_{1g}(^4G)$	22124	22400	22172	21800	22200
$^6A_{1g} \rightarrow {}^4T_{2g}$	—	26509	—		
$^6A_{1g} \rightarrow {}^4E_g$	—	27067	—		
Tetrahedral Fe^{3+}					
$^6A_1 \rightarrow {}^4E, {}^4A_1(^4G)$	23310	23280	23020	23020	23080

* This band may instead be due to the $^6A_{1g} \rightarrow {}^2A_{2g}$ and $^6A_{1g} \rightarrow {}^2T_{1g}$ ligand-field transitions of Fe^{3+}.

3268 cm^{-1}, respectively. These values are comparable to those in other ferric oxides and silicates. In addition to the octahedral Fe^{3+} ligand field bands, there is a broad absorption band centered near 21890 cm^{-1}. This band cannot be due to tetrahedral Fe^{3+}, because its intensity is independent of the fraction of tetrahedral Fe (as indicated by their Mössbauer spectra and structural formulae). There is a similar band in the spectra of ferric oxides and oxide-hydroxides (Sherman and Waite, 1985) that is assigned to the simultaneous excitation of two Fe^{3+} cations to the $^4T_{1g}(^4G)$ ligand field state. Such "double excitation" transitions are expected to occur when next-nearest-neighbor Fe^{3+} cations are magnetically coupled and were first pointed out by Ferguson and Fielding (1972) in the spectrum of Fe^{3+} cations in Al_2O_3. An alternative assignment of the band near 21890 cm^{-1} in both nontronite and the ferric oxides is to the $^6A_1 \rightarrow {}^2T_{1g}$ and $^6A_1 \rightarrow {}^2A_{2g}$ transitions. Neglecting configurational interaction, the ligand-field-theory expressions for the energies of these transitions are (Griffith, 1964)

$$E(^2A_{2g}) = -10Dq + 12B + 9C$$
$$E(^2T_{1g}) = -10Dq + 13B + 9C.$$

Using the calculated values for $10Dq$, B, and C, the energies of the two transitions are predicted to be 21700 cm^{-1} and 22300 cm^{-1}, in excellent agreement with the observed energy of 21890 cm^{-1}. The only way to distinguish between the quintet-triplet transition and the pair-excitation mechanism is by the temperature dependence of the band intensity (Ferguson and Fielding, 1972).

The intensity of the absorption band near 23000 cm^{-1} in the nontronite spectra correlates, at least qualitatively, with the tetrahedral Fe content. The position of this band agrees with that of the $^6A_1 \rightarrow {}^4E, {}^4A_1$ transition of tetrahedrally coordinated Fe^{3+}, as observed for other silicates such as orthoclase (Manning, 1970; White et al., 1986) and phlogopite (Karickhoff and Bailey, 1973; Farmer and Boettcher, 1981). The ligand field transitions of tetrahedrally coordinated Fe^{3+} are Laporte-allowed. Hence, it is reasonable that small amounts (1–4%) of tetrahedral Fe^{3+} should give such a prominant band, because the absorption coefficient for tetrahedrally coordinated Fe^{3+} is 10–100 times that for octahedrally coordinated Fe^{3+}. Assuming this band to be due to tetrahedrally coordinated Fe^{3+}, its intensity is about 50 times that for the analogous $^6A_{1g} \rightarrow {}^4E_g, {}^4A_{1g}$ transition of octahedrally coordinated Fe^{3+}, which is reasonable. There is no evidence, however, for the $^6A_1 \rightarrow {}^4T_1$ and $^6A_1 \rightarrow {}^4T_2$ bands of tetrahedrally coordinated Fe^{3+}. The spectra of oxides (e.g., Waychunas and Rossman, 1983) and silicates containing tetrahedrally coordinated Fe^{3+} show that the absorption bands due to the $^6A_1 \rightarrow {}^4T_1$ and $^6A_1 \rightarrow {}^4T_2$ transitions are much weaker than those associated with the $^6A_1 \rightarrow {}^4E, {}^4A_1$ transition, for reasons that are not understood. Presumably, this difference is why the $^6A_1 \rightarrow {}^4T_1$ and $^6A_1 \rightarrow {}^4T_2$ absorption bands of tetrahedrally coordinated Fe^{3+} cannot be detected (or at least resolved) in the nontronite spectra.

Nontronite is pale apple-green, whereas the ferric oxides and oxide-hydroxides are deep yellow, orange, or red. The absorption band energies in nontronite, however, are very close to those in the ferric oxides and oxide-hydroxides (Sherman and Waite, 1985). The color of nontronite can be explained by noting that the absorption coefficients of the Fe^{3+} ligand field transitions are much smaller for nontronite than for the ferric oxides. As discussed by Sherman and Waite (1985) for the ferric oxides, the Fe^{3+} ligand field transitions are nominally spin-forbidden but can become effectively spin-allowed if next-nearest-neighbor Fe^{3+} cations are magnetically coupled. Strong antiferrogmagnetic coupling between corner-sharing FeO_6 polyhedra in the ferric oxides results in intensification of the Fe^{3+} ligand field transitions. In nontronite, however, FeO_6 polyhedra can only share edges so that the antiferromagnetic coupling is much weaker than in the ferric oxides. The weaker magnetic coupling in nontronite results in a smaller intensification of the Fe^{3+} ligand field transitions, making nontronite pale apple-green as opposed to yellow or red.

A few comments should be made about the origin of the absorption edge in the visible-region spectrum of nontronite. The traditional interpretation of this feature in Fe^{3+}-bearing minerals is that it results from the tail of the lowest-energy $O^{2-} \rightarrow Fe^{3+}$ charge-transfer absorption band. However, it is well known that this transition in nontronite (and other Fe^{3+}-bearing silicates) occurs near 38000 cm^{-1} (e.g., Karickhoff and Bailey, 1973; Sherman, 1985), which is too high in energy to give such a strong absorption edge at 25000 cm^{-1}. To illustrate, a UV–visible region optical-absorption spectrum of an aqueous suspension of nontronite sample N4 is shown in Figure 9. The $O^{2+} \rightarrow Fe^{3+}$ charge-transfer band gives the peak near 260 nm (38000 cm^{-1}). Although this band contributes to some of the absorption in the visible, most of the visible-region absorption edge results from the higher-energy ligand field transitions of octahedrally coordinated Fe^{3+}. The ligand field transitions are strongly intensified by Fe^{3+}-Fe^{3+} magnetic coupling. In the visible-region diffuse-reflectance spectra, most of the absorption edge can

be attributed to the $^6A_{1g} \rightarrow {}^4T_2$ (^4D) band at 26000 cm^{-1} (Fig. 2c).

(Fe^{2+},Fe^{3+})-bearing saponite

The optical spectrum of Fe-bearing saponite (Fig. 7b) is much different from that of nontronite even though the compositions of the two minerals are fairly similar. The Mössbauer spectrum of this sample shows that it contains a significant amount of tetrahedrally coordinated Fe^{3+} and octahedrally coordinated Fe^{2+}. Thus, in the optical spectrum, the presence of Fe^{2+} in the octahedral layer results in Fe^{2+} ligand field bands near 10000 cm^{-1} and a broad band centered near 15000 cm^{-1} that is assigned to $Fe^{2+} + Fe^{3+} \rightarrow Fe^{3+} + Fe^{2+}$ charge transfer. Intervalence charge transfer occurs near 13700 cm^{-1} in the spectrum of reduced nontronite (Anderson and Stucki, 1979; Lear and Stucki, 1987).

The strong band near 23000 cm^{-1} is assigned to the $^6A_1 \rightarrow {}^4E,{}^4A_1$ transition of tetrahedrally coordinated Fe^{3+}, consistent with the high Fe content of the tetrahedral layer (as indicated by the Mössbauer spectrum). The origin of the band near 20500 is not clear. The bands due to Fe^{2+},$Fe^{2+} \rightarrow Fe^{3+}$ charge transfer and tetrahedrally coordinated Fe^{3+} are all Laporte-allowed and completely mask any bands due to the ligand field transitions of octahedrally coordinated Fe^{3+}.

(Fe^{2+},Fe^{3+})-bearing montmorillonite

The optical spectrum of the Fe-bearing montmorillonite sample (Fig. 8b) is dominated by a broad absorption band at 13200 cm^{-1} that, by analogy with the spectrum of chlorite (e.g., Faye, 1968), is assigned to $Fe^{2+} \rightarrow Fe^{3+}$ charge transfer. Bands at 8400 and 10400 cm^{-1} are due to the $^5T_{2g} \rightarrow {}^5E_g$ transition of Fe^{2+} that has been split by the dynamic Jahn-Teller effect. Other bands are found at 16600, 20500, 22600, and 24500 cm^{-1}. Similar sets of absorption bands are found in the spectra of biotite and chlorite (e.g., Faye, 1968). The energies of these bands correlate with the spin-forbidden quintet-triplet transitions of Fe^{2+}. However, in the spectra of Fe^{2+}-bearing silicates in which there is no Fe^{2+}-Fe^{3+} interaction, the quintet-triplet absorption bands are much weaker and very sharp (e.g., Runciman et al., 1973a, 1973b). Intensification and broadening of these transitions in Fe-bearing montmorillonite, chlorite, and biotite are expected to occur via magnetic coupling between adjacent Fe^{2+} and Fe^{3+} cations.

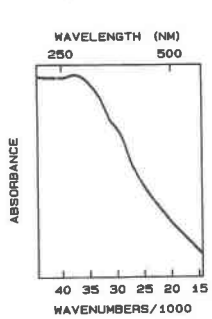

Fig. 9. Near-ultraviolet to visible-region absorption spectrum of an aqueous suspension of nontronite sample N4. The peak near 260 nm (38000 cm^{-1}) is due to the lowest-energy $O^2 \rightarrow Fe^{3+}$ charge-transfer transition. The sharp bands due to the Fe^{3+} ligand field transitions are not well resolved in this spectrum, perhaps owing to light scattering.

Conclusions

Optical spectra of nontronites are dominated by the ligand field transitions of octahedrally coordinated Fe^{3+}. In addition, there is a broad absorption band near 21500 cm^{-1} that is tentatively assigned to the $2[^6A_{1g}] \rightarrow 2[^4T_{1g}]$ pair excitation of magnetically coupled Fe^{3+} cations. Alternatively, this band may result from excitations to the $^2T_{1g}$ and $^2A_{2g}$ states of octahedrally coordinated Fe^{3+} cations. The ligand field transitions of isolated Fe^{3+} cations are spin-forbidden. Magnetic coupling between next-nearest-neighbor Fe^{3+} cations, however, results in an apparent relaxation of the spin-selection rule. The enhancement of the Fe^{3+} ligand field transitions in nontronites is much less than in the spectra of ferric oxides, in accordance with the presumed weaker superexchange coupling between Fe^{3+} cations in nontronite relative to that between Fe^{3+} cations in the ferric oxides. For this reason, nontronites are pale yellow to green rather than orange or red.

Only one set of ligand-field absorption bands due to octahedrally coordinated Fe^{3+} can be resolved from the nontronite spectra. This observation might indicate that Fe^{3+} cations are occupying only the *cis*-$FeO_4(OH)_2$ sites in the octahedral sheet. The ligand fields associated with the *cis*-$FeO_4(OH)_2$ and *trans*-$FeO_4(OH)_2$ coordination sites in the octahedral sheet, however, would be quite similar so that one should not expect to see two sets of Fe^{3+} ligand field bands if the Fe^{3+} cations are occupying both sites.

All of the nontronites show an optical-absorption band near 23000 cm^{-1} that we attribute to the $^6A_1 \rightarrow {}^4E,{}^4A_1$ transition of tetrahedrally coordinated Fe^{3+}. The intensity of this band relative to that of the octahedral Fe^{3+} bands qualitatively increases with the Fe content of the tetrahedral layer determined from the Mössbauer spectra (although the fraction of Fe in tetrahedral coordination is near the limit that can be detected, using Mössbauer spectroscopy, 1–3%). In the optical spectra, the absorption coefficient for the $^6A_1 \rightarrow {}^4E,{}^4A_1$ transition of tetrahedrally coordinated Fe^{3+} is about 50 times greater than that for the analogous $^6A_{1g} \rightarrow {}^4E_g,{}^4A_{1g}$ transition of octahedrally coordinated Fe^{3+}. Because of this difference, optical spectra are much more sensitive to tetrahedral Fe^{3+} than Mössbauer spectra. If the band intensities of the optical spectra could be more precisely calibrated, it seems that optical (diffuse reflectance) spectra should be able to give a quantitative measure of the tetrahedral Fe content in nontronite. Nontronites that appear to have no tetrahedral Fe^{3+} indicated by their structural formulae (assuming Al is partitioned into the tetrahedral layer before Fe) may,

in fact, show evidence for some tetrahedrally coordinated Fe^{3+} in their optical and Mössbauer spectra.

The visible and near-infrared spectra of mixed-valence Fe-bearing smectites show broad absorption bands near 13700 cm^{-1} that are due to $Fe^{2+} \rightarrow Fe^{3+}$ charge transfer. It appears that the Fe^{3+}-Fe^{2+} interaction in these samples enhances the Fe^{2+} ligand field bands near 10000 cm^{-1}. This enhancement, together with the charge-transfer bands, means that small amounts of Fe^{2+} will completely mask any absorption bands due to the ligand field transitions of octahedrally coordinated Fe^{3+}. The effect of Fe^{2+} on the spectra of nontronites might be important to consider when using visible to near-infrared spectra for remote sensing, because small changes in composition may result in large changes in optical spectra.

Note added in proof. In the optical spectra, the calculated fit is superimposed upon the experimental data. In all spectra, however, the fit is so close that one cannot distinguish the calculated spectra from the observed data when the figures are reduced.

Acknowledgments

Gene Whitney and Roger Clark reviewed the initial version of the manuscript. Bob Johnson is thanked for helpful discussions. Thanks are due to Paul Hearn for providing sample S1, Pete Dunn (National Museum of Natural History) for access to samples N4 and M1, and Mac Ross for providing samples NB1, N2, and N5.

References cited

Anderson, W.L., and Stucki, J.W. (1979) Effect of structural Fe^{3+} on the absorption spectra of nontronite suspensions. In M.M. Mortland and V.C. Farmer, Eds., Proceedings of the Sixth International Clay Conference. Developments in Sedimentology, 27, 75–84. Elsevier, Amsterdam.

Besson, G., Bookin, A.S., Dainyak, L.G., Rautureau, M., Tsipursky, S.I., Tchoubar, C., and Drits, B.A. (1983) Use of diffraction and Mössbauer methods for the structural and crystallochemical characterization of nontronites. Journal of Applied Crystallography, 16, 374–383.

Bonnin, D., Calas, G., Suquet, H., and Pezerat, H. (1985) Site occupancy of Fe^{3+} in the Garfield nontronite: A spectroscopic study. Physics and Chemistry of Minerals, 12, 55–64.

Brigatti, M.F. (1982) Hisingerite: A review of its crystal chemistry. In H. Van Olphan and F. Veniale, Eds., Proceedings of the Seventh International Clay Conference. Developments in Sedimentology, 35, 97–110. Elsevier, Amsterdam.

Cardile, C.M., and Johnston, J.H. (1985) Structural studies of nontronites with different iron contents by ^{57}Fe Mössbauer spectroscopy. Clays and Clay Minerals, 33, 295–300.

Daynyak, L.G., and Drits, V.A. (1987) Interpretation of Mössbauer spectra of nontronite, celadonite, and glauconite. Clays and Clay Minerals, 35, 363–372.

Eggleton, R.A., Pennington, J.H., Freeman, R.S., and Threadgold, I.M. (1983) Structural aspects of the hisingerite-neotocite series. Clay Minerals, 18, 21–31.

Farmer, G.L., and Boettcher, A.L. (1981) Petrologic and crystal chemical significance of some deep-seated phlogopites. American Mineralogist, 66, 1154–1163.

Faye, G.H. (1968) The optical absorption spectra of iron in six-coordinated sites in chlorite, biotite, phlogopite, and vivianite. Some aspects of pleochroism in the sheet silicates. Canadian Mineralogist, 9, 403–425.

Ferguson, J., and Fielding, P.E. (1972) The origins of the colours of natural yellow, blue, and green sapphires. Australian Journal of Chemistry, 25, 1371–1385.

Goodman, B.A. (1978) The Mössbauer spectra of nontronites: Consideration of an alternative assignment. Clays and Clay Minerals, 26, 176–177.

Griffith, J.S. (1964) The theory of transition metal ions. University Press, Cambridge.

Helsen, J.A., and Goodman, B.A. (1983) Characterization of iron(II)- and iron(III)-exchanged montmorillonite and hectorite using the Mössbauer effect. Clay Minerals, 18, 117–125.

Jackson, M.L. (1956) Soil chemical analysis—Advanced course. Published by the author, Department of Soil Science, University of Wisconsin, Madison, Wisconsin.

Johnston, J.H., and Cardile, C.M. (1985) Iron sites in nontronite and the effect of interlayer cations from Mössbauer spectra. Clays and Clay Minerals, 33, 21–30.

Karickhoff, S.W., and Bailey, G.W. (1973) Optical absorption spectra of clay minerals. Clays and Clay Minerals, 21, 59–70.

Kinter, E.B., and Diamond, S. (1956) A new method for preparation and treatment of oriented aggregate samples of soil clays for X-ray diffraction analysis. Soil Science, 81, 111–120.

Kohyama, N., Shimoda, S., and Sudo, T. (1973) Iron-rich saponite (ferrous and ferric forms). Clays and Clay Minerals, 21, 229–237.

Lear, P.R., and Stucki, J.W. (1987) Intervalence electron transfer and magnetic exchange in reduced nontronite. Clays and Clay Minerals, 35, 373–378.

Manning, P.G. (1970) Racah parameters and their relationships to lengths and covalencies of Mn^{2+} and Fe^{3+} oxygen bonds in silicates. Canadian Mineralogist, 10, 677–687.

Mering, J., and Oberlin, A. (1967) Electron optical study of smectites. Clays and Clay Minerals, 27, 3–25.

Murad, E. (1987) Mössbauer spectra of nontronites: Structural implications and characterization of associated iron oxides. Zeitschrift Pflanzenernahrung Bodenkunde, 150, 279–285.

Ross, C.S., and Hendricks, S.B. (1945) Minerals of the montmorillonite group and their origin and relations to soils and clays. U.S. Geological Survey Professional Paper 205-B, 79 p.

Runciman, W.A., Sengupta, D., and Marshall, M. (1973a) The polarized spectra of iron in silicates. I. Enstatite. American Mineralogist, 58, 444–450.

Runciman, W.A., Sengupta, D., and Gourley, J.T. (1973b) The polarized spectra of iron in silicates. II. Olivine. American Mineralogist, 58, 451–456.

Sherman, D.M. (1985) Electronic structures of Fe^{3+} coordination sites in iron oxides; applications to spectra, bonding, and magnetism. Physics and Chemistry of Minerals, 12, 161–175.

Sherman, D.M., and Waite, T.D. (1985) Electronic spectra of Fe^{3+} oxides and oxide hydroxides in the near IR to near UV. American Mineralogist, 70, 1262–1269.

Singer, R.B. (1982) Spectral evidence for the mineralogy of the high-albedo soils and dust on Mars. Journals of Geophysical Research, 87, 10159–10168.

Waychunas, G.A., and Rossman, G.R. (1983) Spectroscopic standard for tetrahedrally coordinated ferric iron: $LiAlO_2$:Fe^{3+}. Physics and Chemistry of Minerals, 9, 212–215.

White, W.B., Matsumura, M., Linnehan, D.G., Furukawa, T., and Chandrasekhar, B.K. (1986) Absorption and luminescence of Fe^{3+} in single-crystal orthoclase. American Mineralogist, 71, 1415–1419.

Manuscript received December 18, 1987
Manuscript accepted August 1, 1988